

# Roboflow 100: A Rich, Multi-Domain Object Detection Benchmark

Floriana Ciaglia<sup>\*</sup>, Francesco Saverio Zuppichini<sup>\*</sup>, Paul Guerrie<sup>\*</sup>, Mark McQuade<sup>\*</sup>, and Jacob Solawetz<sup>\*</sup>

<sup>\*</sup>[floriana, paul, francesco, mark, jacob]@roboflow.com

## Abstract

The evaluation of object detection models is usually performed by optimizing a single metric, e.g. mAP, on a fixed set of datasets, e.g. Microsoft COCO and Pascal VOC. Due to image retrieval and annotation costs, these datasets consist largely of images found on the web and do not represent many real-life domains that are being modelled in practice, e.g. satellite, microscopic and gaming, making it difficult to assert the degree of generalization learned by the model.

We introduce the Roboflow-100 (RF100) consisting of 100 datasets, 7 imagery domains, 224,714 images, and 805 class labels with over 11,170 labelling hours. We derived RF100 from over 90,000 public datasets, 60 million public images that are actively being assembled and labelled by computer vision practitioners in the open on the web application [Roboflow Universe](#). By releasing RF100, we aim to provide a semantically diverse, multi-domain benchmark of datasets to help researchers test their model’s generalizability with real-life data. RF100 download and benchmark replication are available on [GitHub](#).

VOC[[Everingham et al., 2010](#)] have become the *de facto* benchmark standards to train and evaluate the performance of models. These models are then released to the public who fine-tuned them on a smaller dataset consisting of specific imagery and targets of interest. While the general object detection benchmarks provide a proxy for how the model will perform in a similar setting, there is no substitute for domain-specific training.

There is a strong research interest in evaluating models on a more diverse task set. For example, 13 Roboflow community open source datasets have organically been used by researchers to create The Object Detection in the Wild (ODINW) [[Li et al., 2021](#)] benchmark. This benchmark was utilized to assert model performance for object detection and zero-shot capabilities in Florence [[Yuan et al., 2021](#)] and GLIP [[Li et al., 2021](#)]. Through curating a larger set of narrow task datasets, we build on this interest for deeper domain-specific assessment and introduce a stronger benchmark we called Roboflow 100 (RF100).

RF100 consists of a collection of 100 crowd-sourced object detection (OD) datasets, specifically constructed by Roboflow users to represent a chosen subject of study. In [Figure 1](#) we show a small sample of annotated image domains that the RF100 benchmark encompasses, which range from satellite and aerial

## 1 Introduction

In object detection research, Microsoft COCO[[Lin et al., 2014](#)] and Pascal

	<i>Aerial</i>	<i>Videogames</i>	<i>Microscopic</i>	<i>Underwater</i>	<i>Documents</i>	<i>Electromagnetic</i>	<i>Real World</i>	<i>COCO</i>
Datasets	7	7	11	5	8	12	50	1
Images	9683	11579	13378	18003	24813	36381	110615	328000
Classes	24	88	28	39	90	41	495	80
YOLOv5	0.636	0.859	0.650	0.560	0.716	0.689	0.752	0.568
YOLOv7	0.504	0.796	0.591	0.662	0.722	0.607	0.699	0.697
GLIP	0.23	0.188	0.159	0.019	0.024	0.058	0.108	0.466

Table 1: Overview of per-category metadata, including number of datasets, number of images, and number of classes across categories. Additionally, we record the average mAP@.50 value for the YOLOv5 and YOLOv7 models and the mAP@.50:.95 for the GLIP model for each category.

assessment to microscopic image analysis.

By introducing a benchmark of narrow subject matter datasets, we accomplish two goals. Firstly, our benchmark provides a strong collection of closed-domain tasks used in the wild that are of demonstrated interest to practitioners for researchers that are designing models with the intent of them being fine-tuned. Secondly, researchers building general models can test transfer between object detection tasks in zero-shot or few-shot fashion.

## 2 Related Work

Historically, object detection datasets are created by gathering a large corpus of images and sourcing annotators to label objects in a fixed set of classes.

The Pascal VOC project [Everingham et al., 2010] is a collection of datasets made to enhance object detection tasks and encourage researchers to create models that recognize objects in realistic scenes in the form of a challenge. The Pascal VOC challenges started in 2005 and laid the groundwork for a new generation of state-of-the-art benchmarks.

ImageNet [Deng et al., 2009] is an image dataset comprised of over 14 million images each described by word phrases called "synset". It was specifically created to answer the need in the industry for a high-quality object categorization benchmark with clearly established evaluation metrics. Similarly to RF100, ImageNet was created to encourage the creation of more generalizable machine learning models.

Open Images [Kuznetsova et al., 2020] is an image collection with over 9 million annotated images and 600 object classes. It was created to enable the study of tasks such as image classification, object detection, visual relationship detection, instance segmentation, and multi-modal image descriptions all from one joined resource to stimulate progress towards image scene comprehension.

The Common Objects in Context [Lin et al., 2014] (COCO) benchmark is a large-scale object detection and segmentation dataset with a total of 2.5M labelled instances in 328K images. Ever since its release, the COCO benchmark has established itself as the state-of-the-

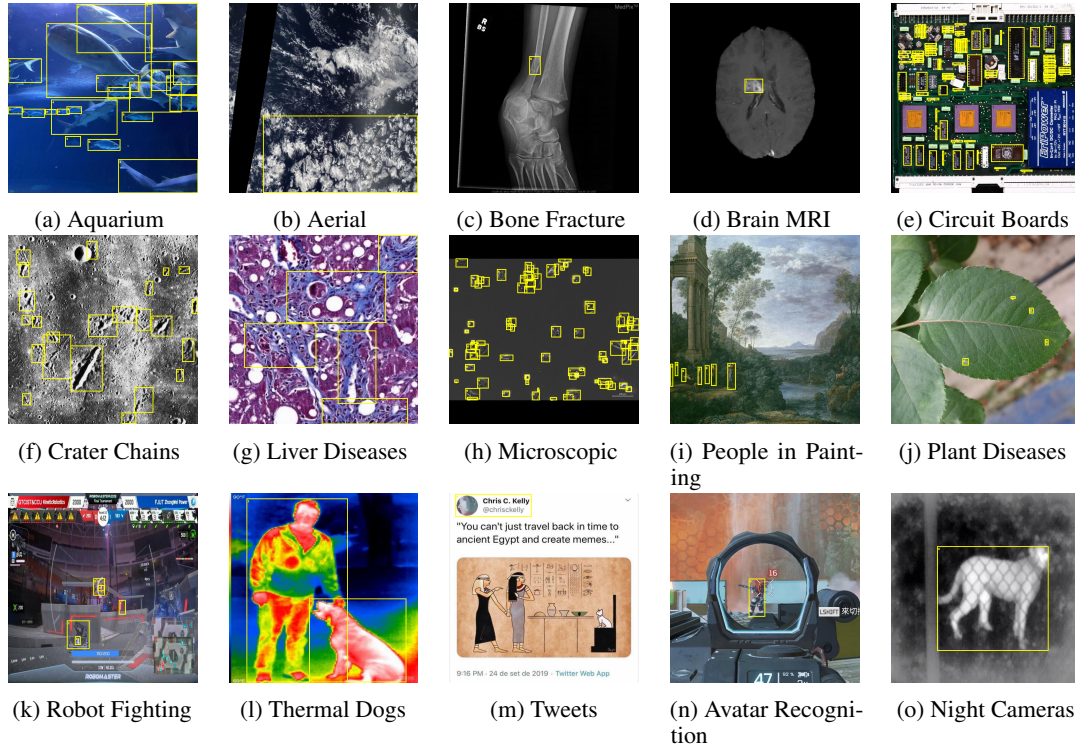


Figure 1: Examples of annotated images in the RF100 benchmark. The data-set names are derived from the object of interest of each collection. Further examples can be found in Appendix A

art standard thanks to its abundance of subjects and annotations.

The Objects365 [Shao et al., 2019] dataset is a large collection of separate object detection datasets that is comprised of images from the website Flickr. Images are gathered, categories are assigned, and then a labelling team is employed to create annotations. Pretraining models on Objects365 are shown to benefit performance on downstream tasks, such as COCO.

The Object Detection in the Wild (ODINW) [Li et al., 2021] dataset was released in the same spirit as RF100. The original ODINW version uses 13 Roboflow object detection datasets to assess the generalizability of their zero-shot model, GLIP [Li et al., 2021]. Despite advances in open vocabulary object detectors like GLIP, accurate and fast object de-

tection still requires custom training to be performed on quality, annotated data with a closed vocabulary.

Unlike prior related work, we assemble a large-scale object detection dataset that is sourced via image upload and annotation by practitioners on a web application who are using computer vision to accomplish real tasks.

### 3 Methods

In this section, we describe the RF100 dataset creation process and our initial modelling experiments on the new benchmark.

#### 3.1 Dataset Collection and Distribution

Roboflow Universe is a public repository of computer vision dataset that over 100,000 Roboflow users have assembled and labeled

for their own custom use cases. We selected 100 datasets from [Roboflow Universe](#) for our benchmark using the following criteria:

- Effort - the user spent substantial labelling hours working on the task;
- Diversity - the user was working on a novel task;
- Quality - the user annotated with high fidelity to the task;
- Substance - the user assembled a substantial dataset with nuance;
- Feasibility - the user was attempting a learnable task;

After selection for inclusion, all datasets were processed in the following way:

- All images resized to 640x640 pixels following best practices [[Wang et al., 2022](#)]
- Eliminate class ambiguity, i.e. if a class was labeled by the original author as *0* to represent a flower, that class label would be changed to a word descriptive of the actual subject such as *daisy*
- The train, validation, and test split were manipulated only in the instances where either one or more split sets were missing completely, or where one, or more, of the split sets were extremely under-represented. In all other cases, we respected the split ratio chosen by the original author of the dataset.
- Underrepresented classes were filtered when they represented less than 0.5 percent of all objects in a dataset. These classes tended to be labeling errors.

The datasets are available for download from [GitHub](#) or from the [Roboflow Universe website](#) by clicking on the *Export* button.

Category	Datasets	Images	Classes
Aerial	7	9683	24
Videogames	7	11579	88
Microscopic	11	13378	28
Underwater	5	18003	39
Documents	8	24813	90
Electromagnetic	12	36381	41
Real World	50	110615	495
<b>Total</b>	<b>100</b>	<b>224,714</b>	<b>805</b>

Table 2: Overview of per-category metadata, including number of datasets, number of images, and number of classes across categories.

### 3.2 Semantics

We selected seven different semantic categories to achieve comprehensive coverage of real-life possible domains: Aerial, Video Games, Microscopic, Underwater, Documents, Electromagnetic and Real World.

The Real World category is the biggest in the RF100 benchmark since the majority of use cases for computer vision involve everyday scenes. We included indoor, outdoor, Vehicles, animals, plants, damage control, safety, electronics, geology, board games and various human activity images.

The Video Games category includes virtual reality scenes, robot fighting, first-person shooters and MOBA; The Underwater category includes fishery sights from both seas and aquariums, as well as inanimate objects found underwater (i.e. pipes).

The Microscopic category is comprised of items that can only be seen with the aid of a microscopic lens like bacteria and human cells; the Aerial category includes images taken from an overhead view, including images from space and drones; the Electromagnetic category includes scenarios where electromagnetic waves were used to capture the



pictures, X-rays, MRIs, IR, thermal and night vision cameras; and finally, in the Documents category, we include all images that relate to articles, papers, tables, diagrams and social media.

Figure 4 shows samples for each category.

### 3.3 Data Statistics and Analysis

Table 2 summarizes the benchmark’s metadata including the number of datasets, images and classes present in each category. Per dataset statistics and results can be seen in Table 4.

Figure 2 reports different statistics grouped by category, such as number of classes and bounding boxes area. Most notably, *Aerial*, *Microscopic* and *Electromagnetic* have smaller bounding boxes compared to the rest. Moreover, the average number of classes across different categories is only ten, meaning in practice people need to identify a small set of objects.

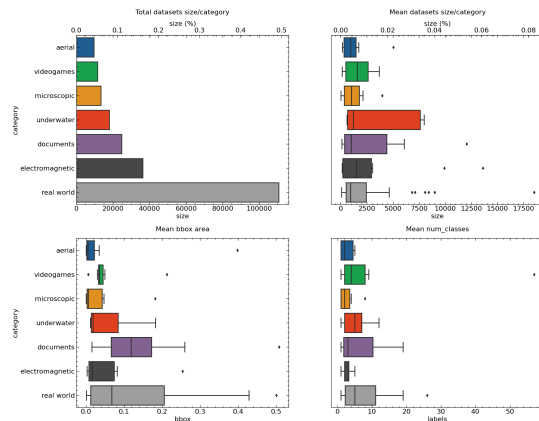


Figure 2: This figure shows different statistics for datasets grouped by category. Noticeably we can notice some categories (aerial, video games) have generally smaller bounding boxes compares to others, like documents. The number of classes is low, averaging 10.

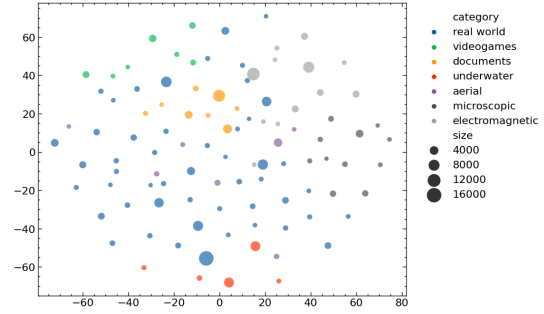


Figure 3: Scatter plot visualization of Roboflow-100 datasets CLIP vectors reduced to two dimensions via TSNE. The graph legend on the top right corner shows what category of dataset each color denotes. This visualization helps us determine the clustering degree of our collected datasets.

Figure 3 shows a scatter plot produced to analyze the vector clustering degree of the RF100 categories using CLIP embeddings [Radford et al., 2021] generates for each of its datasets. This illustration shows that the datasets in each category do tend to cluster together. You can also view an image-level clustering of these semantics on the [RF100 web exploration web demo](#).

### 3.4 Experiments and Evaluation

We trained popular object detection model architectures on RF100 and report the results. Only one model instance was trained per dataset.

**Finetuning:** We finetuned two comparable versions of YOLOv5 [Jocher et al., 2020] and YOLOv7 [Wang et al., 2022]: YOLOv5s and YOLOv7, with 7.2M parameters and 36.9M parameters respectively and similar FPS when evaluated on a Tesla V100.

We trained both models with default hyperparameters for 100 epochs at 640x640 resolution.

**Zero Shot:** We also evaluated GLIP [Li et al., 2022], a zero-shot detector that can solve open vocabulary detection by rephrasing it as

Category	YOLOv5	YOLOv7	GLIP
Aerial	0.636	0.504	0.230
Videogames	0.859	0.796	0.188
Microscopic	0.650	0.591	0.159
Underwater	0.560	0.662	0.019
Documents	0.716	0.722	0.024
Electromagnetic	0.689	0.607	0.058
Real World	0.752	0.699	0.108
<b>Total</b>	<b>0.694</b>	<b>0.654</b>	<b>0.112</b>

Table 3: Experiments results on RF100. We recorded the average mAP@.50 value for the YOLOv5 and YOLOv7 models and the mAP@.50:.95 for the GLIP model for each category.

a grounding task, in which each noun in a sentence is associated with an object in an image.

GLIP’s default behaviour for the evaluation task is to use the objects’ class names as the evaluation prompts. We recognize that some of the RF100 datasets might not have very descriptive class names and that our imagery is, as intended, more specific than other more general benchmarks. As a consequence, we believe that providing GLIP with word phrases to describe the objects in our images would be a more fair challenge for a zero-shot model. We compiled a list of descriptions that match each class for most of the datasets in Roboflow-100. The datasets we did not include in the prompt remapping already had sensible class names.

We evaluate RF100 on the GLIP-T model pre-trained on O365, GoldG, Conceptual Captions 3M, and SBU captions [Li et al., 2022].

Results are reported in Table 3.

## 4 Discussion

Our initial benchmarks show that there is variation in model performance between models across datasets and datasets domains that may

run contrary to the model’s ranking on incumbent benchmarks. A given model may perform better on one dataset and worse on another. While we do not investigate the underlying reasons for performance differentials, our results suggest that there are likely significant improvements to be made to object detection models to expect a wider array of custom datasets that they may be applied to.

Lastly, our evaluation shows that zero-shot object detection models lose considerable performance when extended to new domains. While evaluation on COCO shows that zero-shot models like GLIP are approaching the performance of their fine-tuned counterparts, our benchmark shows that they do not generalize well to new, more obscure imagery domains. This is likely due to the out-of-vocabulary imagery types and class titles from what frequently appears in image datasets assembled on the web.

## 5 Conclusion

We introduce the RF100 object detection benchmark of 100 datasets to encourage the evaluation of object detection model performance to test model generalizability across a wider array of imagery domains. Our initial evaluation shows that the new RF100 benchmark will provide valuable insights into how new object detection models will perform in the wild. RF100 is available for download on [GitHub](#).

## Acknowledgments

We thank all of the advisors we have had on our research both internally at Roboflow, and externally in the machine learning community. We would also like to thank Intel for sponsoring the work involved in constructing the RF100 benchmark.

Finally, we thank everyone working on public computer vision datasets on Roboflow

Universe and in particular, the creators of the RF100 datasets: Abhishek Dada, Adam Crenshaw, Adrian Rodriguez, Ahmad Rabeie, Alex Hyams, Aman Ahuja and Alan Devera, Ammar Abdulmutalib, Amro, Anshul Rankawat, Kapil Verma, Shubhankar Rawat, Manisa Mondal, Pranav Arora, Arfiani Nur Sayidah, Brad Dwyer, Brad Dwyer, CC Moon, Chang Yuan, Dane Sprsiter, David Lee, Djamel Mekhlouf, Abrisse Cerine, Anfal Lanna, Yasmin Emekhlouf, Evan Kim, MJ Kim, Graham Doerksen, Ilyes Talbi, Jan Douwe, Jason Zhang, Caden Li, Jhonathann, Joao Paulo Martins, Jordan Bird, Leah Bird, Carrie Ijichi, Aurelie Jolivald, Salisu Wada, Kay Owa, Chloe Barnes, Joseph Nelson, Brad Dwyer, and Cheng Hsun Teng , Justin Henke, Reginald Viray, Kais Al Hajjih, Karen Weiss, Kat Laura, Lao and Shiguang, Lukas D. Ringle, Matteo Pacini, Melanie S. Capalungan, B-Jay Daguio, Isaac Balbuena, and Reanne Joy Rafael, Mevil Crasta, Miguel Fernández Cruchaga, Mike Drickramer, Minoj Selvaraj, Mohamed Attia, Mohamed Refai, Abarna, Amjad Hafiz, Sutheshan Maiu, and Thanusha Sritharan, Mohamed Sabek, Monika Patel, Kartik Attri, Aniket Dhanotia, Divyam Jha, Pankaj, kanchan, Ujjwal Sharma, Garvita Vijay, Aniket Choudhary, Pearl Rathour, Roshni Ghai, Kavya Shukla, Preeti Sharma, Ananya Kharayat, Krishna Gambhir, Lav Naruka, Kas, Sejal, Tejasvi Singh, Ayush Sahu, Pri, Aniket Dhanotia, and Devansh Shrivastava , Montso Mokake, Muntaser Al Abdulla Aljouma, Nazmuj Shakib Diip, Afraim, Shiam Prohdan, NhiNguyen and Duong Duc Cuong , Nikita Manolis, Nirav Golyalla, Ali Fakhry, Ammar F, Shangyu, Nirmani, Oliver Giesecke, Christian Green, Omar Kapur, Ricardo Jenez, Justin Jeng, and Jeffrey Day, Pablo Ochoa, Antonio Luna, Eliezer Alvarez, Paper Authors, Parfait Ahouanto, Pavel Kulikov, Djopa Volosata, Daria Podryadova, Pierrick Dossin,

Ploylada Pharikarn, Potae, Phuthanig Aree-sawangkit, Prakasit, Tanchanok Prasootseangjan, Quandong Qian, Raya Al, Riccardo Secoli, Kaspars Sudars, Janis Jasko, Ivars Namat-evs, Liva Ozola, and Niks Badaukis, Richard, Rik Biswas, Aakansha Prasad, Sarmistha Das, Rinat Landman, Ritesh Kanjee, Roopa Shree, Shriya J, Ruud Krinkels, Seokjin Ko, Simeon Marlokov, Sina, St Hedgehog Yusupov, T, Pankaj, Aniket Dhanotia, Tejasvi Singh, Garvita Vijay, Goku, Kavya Shukla, Aniket Choudhary, Ananya Kharayat, Monika Patel, Pearl Rathour, Devansh Shrivastava, Aniket Dhanotia, Priyansh Urajput, Sejal, Roshni Ghai, Krishna Gambhir, Ayush Sahu, Ujjwal Sharma, Divyam Jha, Kanchan, Kartik Attri, Lav Naruka, Kas, Preeti Sharma, Terada Shoma, Thuan Phat Nguyen, Vanitchaporn, Victor Perez, Stephen Groff, Mason Hintermeister, Wang Tianyi, Wilfred Shu and Adrian Stuart, Wojciech Blachowski, Wojciech Przydzial, Dorota Przydzial, Magdalena Przydzial-Mazur, and Bartlomiej Mazur, Xingwei He, Yilong Zheng, Yimin Chen, Yousef Ghanem, Yuanyu Anpei, Yudha Bhakti Nugraha and Kris, Yuntaewon, Hwanghyeyun, Gimminseo, Gimnohyeon , Sindahong, Gimseongsu, Yuyang Li, Zhang Kaimin, Zhe Fan.

## References

- Jia Deng, Wei Dong, Richard Socher, Li-Jia Li, Kai Li, and Li Fei-Fei. Imagenet: A large-scale hierarchical image database. In *2009 IEEE conference on computer vision and pattern recognition*, pages 248–255. Ieee, 2009.
- Mark Everingham, Luc Van Gool, Christopher K. I. Williams, John M. Winn, and Andrew Zisserman. The pascal visual object classes (voc) challenge. *Int. J. Comput. Vis.*, 88(2):303–338, 2010. URL <http://dblp.uni-trier.de/db/journals/ijcv/ijcv88.html#EveringhamGWZ10>.
- Glenn Jocher, Alex Stoken, Jirka Borovec, NanoCode012, ChristopherSTAN, Liu Changyu, Laughing, tkianai, Adam Hogan, lorenzomamma, yxNONG, AlexWang1900, Laurentiu Diaconu, Marc, wanghaoyang0106, ml5ah, Doug, Francisco Ingham, Frederik, Guilhen, Hatovix, Jake Poznanski, Jiacong Fang, Lijun Yu, changyu98, Mingyu Wang, Naman Gupta, Osama Akhtar, PetrDvoracek, and Prashant Rai. ultralytics/yolov5: v3.1 - Bug Fixes and Performance Improvements, October 2020. URL <https://doi.org/10.5281/zenodo.4154370>.
- Alina Kuznetsova, Hassan Rom, Neil Alldrin, Jasper Uijlings, Ivan Krasin, Jordi Pont-Tuset, Shahab Kamali, Stefan Popov, Matteo Mallocci, Alexander Kolesnikov, Tom Duerig, and Vittorio Ferrari. The open images dataset v4: Unified image classification, object detection, and visual relationship detection at scale. *IJCV*, 2020.
- Liunian Harold Li, Pengchuan Zhang, Haotian Zhang, Jianwei Yang, Chunyuan Li, Yiwu Zhong, Lijuan Wang, Lu Yuan, Lei Zhang, Jenq-Neng Hwang, Kai-Wei Chang, and Jianfeng Gao. Grounded language-image pre-training, 2021. URL <https://arxiv.org/abs/2112.03857>.
- Liunian Harold Li, Pengchuan Zhang, Haotian Zhang, Jianwei Yang, Chunyuan Li, Yiwu Zhong, Lijuan Wang, Lu Yuan, Lei Zhang, Jenq-Neng Hwang, et al. Grounded language-image pre-training. In *Proceedings of the IEEE/CVF Conference on Computer Vision and Pattern Recognition*, pages 10965–10975, 2022.
- Tsung-Yi Lin, Michael Maire, Serge Belongie, Lubomir Bourdev, Ross Girshick, James Hays, Pietro Perona, Deva Ramanan, C. Lawrence Zitnick, and Piotr Dollár. Microsoft coco: Common objects in context, 2014. URL <https://arxiv.org/abs/1405.0312>.
- Alec Radford, Jong Wook Kim, Chris Hallacy, Aditya Ramesh, Gabriel Goh, Sandhini Agarwal, Girish Sastry, Amanda Askell, Pamela Mishkin, Jack Clark, Gretchen Krueger, and Ilya Sutskever. Learning transferable visual models from natural language supervision, 2021. URL <https://arxiv.org/abs/2103.00020>.
- Shuai Shao, Zeming Li, Tianyuan Zhang, Chao Peng, Gang Yu, Xiangyu Zhang, Jing Li, and Jian Sun. Objects365: A large-scale, high-quality dataset for object detection. In *2019 IEEE/CVF International Conference on Computer Vision (ICCV)*, pages 8429–8438, 2019. doi: 10.1109/ICCV.2019.00852.
- Chien-Yao Wang, Alexey Bochkovskiy, and Hong-Yuan Mark Liao. YOLOv7: Trainable bag-of-freebies sets new state-of-the-art for real-time object detectors, 2022.
- Lu Yuan, Dongdong Chen, Yi-Ling Chen, Noel Codella, Xiyang Dai, Jianfeng Gao, Houdong Hu, Xuedong Huang, Boxin Li, Chunyuan Li, Ce Liu, Mengchen Liu, Zicheng Liu, Yumao Lu, Yu Shi, Lijuan Wang, Jianfeng Wang, Bin Xiao, Zhen Xiao, Jianwei Yang, Michael Zeng, Luowei Zhou, and Pengchuan Zhang. Florence: A new foundation model for computer vision, 2021. URL <https://arxiv.org/abs/2111.11432>.



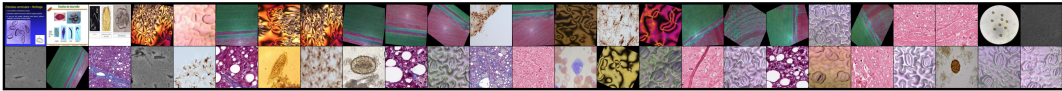
## A Appendix



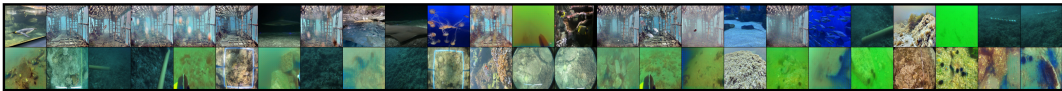
(a) **Areal** images gather from drone, space and static cameras



(b) **Video Games** screen recordings from different games, such as Far Cry, Apex Legends, CS Go and League of Legends.



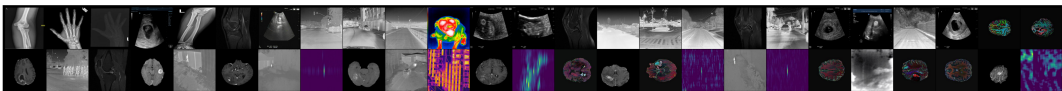
(c) **Microscopic** images, mostly human diseases recorded with medical equipment showing cells, parasites, bacteria.



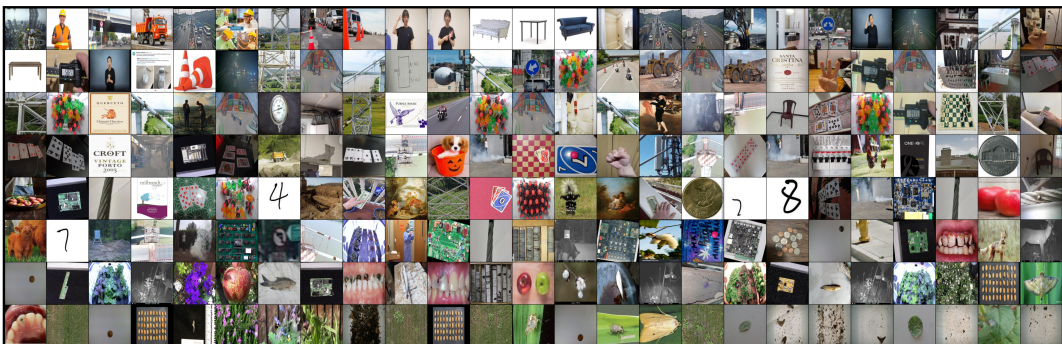
(d) **Underwater** images of various sea plants and animals collected in the sea or aquariums.



(e) **Documents** such as tweets, tables and activity diagrams.



(f) **Electromagnetic** images from X-ray, thermal cameras and MRI.



(g) **Real World** images from a wide array of domains, animals, vehicles, human activities, paintings and electronics.

Figure 4: Examples of images samples from different categories. *Real World* was sampled more due to its bigger size.



Dataset	Category	Images			Labeling		YOLOv5	YOLOv7	GLIP
		Train	Valid	Test	Hours	Classes	mAP@.50	mAP@.50	mAP@.50:.95
aerial pool	aerial	673	96	177	421	7	0.513	<b>0.791</b>	0.013
secondary chains	aerial	103	16	43	201	1	<b>0.341</b>	0.312	0.000
aerial spheres	aerial	318	51	104	177	6	<b>0.993</b>	0.539	0.000
soccer players	aerial	114	16	33	0	3	<b>0.660</b>	0.399	0.065
weed crop	aerial	823	118	235	0	2	<b>0.820</b>	0.615	0.027
aerial cows	aerial	1084	299	340	179	1	<b>0.854</b>	0.568	0.056
cloud types	aerial	3528	504	1008	0	4	0.271	<b>0.306</b>	0.006
apex videogame	videogames	2583	415	691	-1	2	0.839	<b>0.875</b>	n/a
farcry6 videogame	videogames	82	14	24	0	11	<b>0.619</b>	0.216	0.248
csgo videogame	videogames	1774	207	446	0	2	<b>0.974</b>	0.964	0.184
avatar recognition	videogames	225	30	59	3	1	0.889	<b>0.943</b>	0.367
halo infinite	videogames	462	71	136	4	4	0.921	<b>0.924</b>	0.173
team fight	videogames	1162	112	307	88	59	<b>0.961</b>	0.880	0.000
robomasters 285km	videogames	1945	278	556	27	9	<b>0.816</b>	0.772	0.003
stomata cells	microscopic	1482	209	414	0	2	0.840	<b>0.847</b>	0.012
bccd ouzjz	microscopic	255	36	73	0	3	0.912	<b>0.922</b>	0.191
parasites 1s07h	microscopic	1484	215	411	0	8	0.848	<b>0.889</b>	0.036
cells uyemf	microscopic	16	2	4	210	1	<b>0.249</b>	0.085	0.005
4 fold	microscopic	503	33	134	279	1	<b>0.970</b>	0.938	0.000
bacteria ptywi	microscopic	30	10	10	472	1	<b>0.162</b>	0.001	0.000
cotton plant	microscopic	724	102	198	259	1	<b>0.204</b>	0.052	0.000
mitosis gjs3g	microscopic	213	30	61	0	1	<b>0.931</b>	0.739	0.001
phages	microscopic	1155	103	164	74	2	<b>0.854</b>	0.842	0.002
liver disease	microscopic	2782	400	794	31	4	<b>0.592</b>	0.583	0.000
asbestos	microscopic	932	133	266	126	4	0.596	<b>0.611</b>	0.007
underwater pipes	underwater	5617	779	1575	316	1	0.995	<b>0.998</b>	0.733
aquarium qlnqy	underwater	448	63	127	0	7	0.790	<b>0.822</b>	0.195
peixos fish	underwater	821	118	261	0	12	0.148	<b>0.821</b>	0.004
underwater objects	underwater	5320	760	1520	0	5	<b>0.693</b>	0.453	0.005
coral lwptl	underwater	427	74	93	165	14	0.174	<b>0.218</b>	0.001
tweeter posts	documents	87	9	21	0	2	<b>0.708</b>	0.495	0.005
tweeter profile	documents	425	61	121	0	1	0.988	<b>0.990</b>	0.002
document parts	documents	906	150	318	192	2	<b>0.677</b>	0.666	0.033
activity diagrams	documents	259	45	74	192	19	0.427	<b>0.509</b>	0.002
signatures xc8up	documents	257	37	74	0	1	<b>0.961</b>	0.932	0.082
paper parts	documents	8472	1209	2359	211	46	0.590	<b>0.796</b>	0.007
tabular data	documents	3251	206	409	271	12	0.752	<b>0.782</b>	0.018
paragraphs co84b	documents	4209	633	1221	228	7	<b>0.626</b>	0.610	0.000
thermal dogs	electromagnetic	142	20	41	-1	2	<b>0.967</b>	0.957	0.470
solar panels	electromagnetic	112	19	30	175	5	<b>0.413</b>	0.261	0.000
radio signal	electromagnetic	1954	278	566	0	2	<b>0.673</b>	0.653	0.066

thermal cheetah	electromagnetic	90	14	25	0	2	<b>0.931</b>	0.513	0.028
x ray	electromagnetic	135	16	34	16	12	<b>0.722</b>	0.506	0.000
acl x	electromagnetic	2141	306	612	0	1	0.995	<b>0.998</b>	0.000
abdomen mri	electromagnetic	1887	238	479	0	1	<b>0.965</b>	0.958	0.021
axial mri	electromagnetic	253	39	79	0	2	<b>0.638</b>	0.549	0.039
gynecology mri	electromagnetic	2122	253	526	7	3	<b>0.323</b>	0.171	0.000
brain tumor	electromagnetic	6930	990	1980	0	3	0.768	<b>0.809</b>	0.003
bone fracture	electromagnetic	326	44	88	0	4	0.085	<b>0.090</b>	0.000
flir camera	electromagnetic	9306	1452	2854	17	4	0.796	<b>0.824</b>	0.073
hand gestures	real world	642	94	178	-1	14	<b>0.995</b>	0.995	n/a
smoke uvylj	real world	522	76	148	7	1	0.959	<b>0.962</b>	0.431
wall damage	real world	325	40	96	-1	3	<b>0.500</b>	0.434	n/a
corrosion bi3q3	real world	840	105	304	186	3	<b>0.768</b>	0.764	0.003
excavators czvg9	real world	2244	144	267	0	3	<b>0.946</b>	0.895	0.274
chess pieces	real world	202	29	58	0	13	<b>0.977</b>	0.830	0.017
road signs	real world	1376	229	488	0	21	<b>0.963</b>	0.944	0.036
street work	real world	611	87	175	2	11	0.478	<b>0.708</b>	0.148
construction safety	real world	997	90	119	505	5	<b>0.915</b>	0.915	0.259
road traffic	real world	494	133	187	-1	12	0.597	<b>0.847</b>	n/a
washroom rf1fa	real world	1885	318	775	449	10	0.619	<b>0.634</b>	0.146
circuit elements	real world	672	36	64	311	46	<b>0.063</b>	n/a	0.001
mask wearing	real world	105	15	29	0	2	<b>0.788</b>	0.513	0.008
cables nl42k	real world	4816	794	1220	0	11	0.688	<b>0.722</b>	0.010
soda bottles	real world	1547	216	486	243	6	<b>0.964</b>	n/a	0.098
truck movement	real world	740	107	215	282	7	0.786	<b>0.846</b>	0.007
wine labels	real world	3172	630	841	249	12	0.569	<b>0.632</b>	0.045
digits t2eg6	real world	2912	367	824	144	10	<b>0.989</b>	0.989	0.003
vehicles q0x2v	real world	2634	458	966	1121	-1	0.454	<b>0.464</b>	0.029
peanuts sd4kf	real world	268	42	77	212	2	0.995	<b>0.997</b>	0.358
printed circuit	real world	548	44	80	311	34	<b>0.091</b>	n/a	0.000
pests 2xlvx	real world	509	55	153	188	28	<b>0.136</b>	0.029	0.004
cavity rs0uf	real world	287	38	93	165	2	0.782	<b>0.799</b>	0.029
leaf disease	real world	1589	296	616	143	3	0.531	<b>0.560</b>	0.027
marbles	real world	54	32	19	133	2	<b>0.992</b>	0.473	0.030
pills sxdht	real world	316	45	90	0	8	<b>0.869</b>	0.867	0.194
poker cards	real world	964	128	193	0	53	<b>0.886</b>	0.251	-0.000
number ops	real world	4869	623	1636	28	15	0.990	<b>0.992</b>	0.055
insects mytwu	real world	696	100	199	0	10	<b>0.890</b>	0.858	0.024
cotton 20xz5	real world	367	20	19	17	4	0.569	<b>0.591</b>	0.157
furniture ngpea	real world	454	74	161	0	3	<b>0.983</b>	0.968	0.836
cable damage	real world	919	134	265	2	2	<b>0.910</b>	0.574	0.006
animals ij5d2	real world	700	100	200	12	10	<b>0.761</b>	0.342	0.249
coins lapki	real world	6121	699	1599	0	4	0.932	<b>0.977</b>	0.175
apples fvp15	real world	489	30	178	-1	2	0.779	<b>0.791</b>	n/a

people in	real world	634	81	194	5	1	0.575	<b>0.678</b>	0.168
circuit voltages	real world	92	15	25	11	6	<b>0.797</b>	0.257	0.009
uno deck	real world	6295	899	1798	0	15	0.993	<b>0.994</b>	0.013
grass weeds	real world	1661	245	580	105	1	<b>0.781</b>	0.781	0.106
gauge u2lwv	real world	158	25	52	141	2	0.642	<b>0.668</b>	0.217
sign language	real world	504	72	144	0	26	<b>0.870</b>	0.255	0.006
valentines chocolate	real world	68	6	13	4	22	<b>0.110</b>	0.059	0.013
fish market	real world	14180	1202	3116	252	21	0.920	<b>0.988</b>	0.013
lettuce pallets	real world	1060	151	299	168	5	0.945	<b>0.966</b>	0.031
shark teeth	real world	191	36	53	154	4	<b>0.948</b>	0.863	0.025
bees jt5in	real world	5640	836	1604	163	1	<b>0.891</b>	0.680	0.009
sedimentary features	real world	156	21	45	31	5	<b>0.327</b>	0.244	0.000
currency v4f8j	real world	576	82	155	1	10	<b>0.583</b>	0.514	0.099
trail camera	real world	941	131	239	4	2	0.966	<b>0.969</b>	0.512
cell towers	real world	705	101	202	25	2	0.939	<b>0.942</b>	0.053

Table 4: The above table reports metadata about each dataset in RF100. It includes each data-set’s name, number of classes, labeling hours spend by the original author, the train/validation/test split used, model’s mAP@.50 value on the three bench marked models and the source link. In the labeling hours column, a zero value denotes that the dataset was annotated outside of the Roboflow app, and a *n/a* value denotes that the dataset was created before Roboflow started keeping track of the labeling hours data.